Spatial regulation of Raf kinase signaling by RKTG

Lin Feng, Xiaoduo Xie, Qiurong Ding, Xiaolin Luo, Jing He, Fengjuan Fan, Weizhong Liu, Zhenzhen Wang, and Yan Chen*

Institute for Nutritional Sciences, Shanghai Institutes for Biological Sciences, Chinese Academy of Sciences, Graduate School of the Chinese Academy of Sciences, Shanghai 200031, China

Edited by Melanie H. Cobb, University of Texas Southwestern Medical Center, Dallas, TX, and approved July 18, 2007 (received for review February 12, 2007)

Subcellular compartmentalization has become an important theme in cell signaling such as spatial regulation of Ras by RasGRP1 and MEK/ERK by Sef. Here, we report spatial regulation of Raf kinase by RKTG (Raf kinase trapping to Golgi). RKTG is a seven-transmembrane protein localized at the Golgi apparatus. RKTG expression inhibits EGF-stimulated ERK and RSK phosphorylation, blocks NGF-mediated PC12 cell differentiation, and antagonizes Ras- and Raf-1-stimulated Elk-1 transactivation. Through interaction with Raf-1, RKTG changes the localization of Raf-1 from cytoplasm to the Golgi apparatus, blocks EGF-stimulated Raf-1 membrane translocation, and reduces the interaction of Raf-1 with Ras and MEK1. In RKTG-null mice, the basal ERK phosphorylation level is increased in the brain and liver. In RKTG-deleted mouse embryonic fibroblasts, EGF-induced ERK phosphorylation is enhanced. Collectively, our results reveal a paradigm of spatial regulation of Raf kinase by RKTG via sequestrating Raf-1 to the Golgi apparatus and thereby inhibiting the ERK signaling pathway.

EGF | ERK | Golgi | Raf-1 | Ras | PAQR3

Raf kinase relays the signals from Ras to MEK (MAPK and ERK kinase) and ERK/MAPK (1, 2). This pathway regulates many fundamental cellular functions, including cell proliferation, apoptosis, differentiation, motility, and metabolism, and is implicated in many human diseases including cancer (3). In the Ras/Raf/MEK/ERK signaling cascade, several players within this pathway are exquisitely regulated by subcellular compartmentalization (4, 5). Kinase suppressor of Ras (KSR) is a scaffold protein that coordinates the assembly of multiprotein MAPK complex in plasma membrane (6). β-Arrestin could also function as a scaffold protein to target the MAPK protein complex to early endosome (7). Different lipid anchors are able to shuttle Ras between different membrane compartments to modulate subcellular Ras signaling (8–10). In T lymphocyte, Ras could be activated *in situ* on the Golgi apparatus via the Ras exchange factor RasGRP1, which is activated by phospholipase C (11). Compartmentalized signaling of Ras/MAPK in T lymphocyte on either plasma membrane or Golgi apparatus leads to distinct output of ERK activation and thereby determines the threshold of thymic selection (12). MEK could be targeted to endosome by a scaffold protein MP1 through adaptor p14 (13). It was also found that MEK/ERK can be recruited to the Golgi by Sef, and that such spatial regulation blocks the Ras signaling to the nucleus but not to the cytosol (14). However, how Raf is regulated in a spatial manner has not been characterized.

The activity of Raf kinase is mainly regulated by phosphorylation events and scaffold proteins (1, 2). In addition, Raf could be negatively regulated by interaction with other proteins. Raf kinase inhibitor protein (RKIP) is able to interact with Raf-1, MEK, and ERK (15). RKIP blocks Raf-1 signaling to MEK by competitively disrupting the interaction between Raf-1 and MEK because both Raf-1 and MEK bind to overlapping sites in RKIP (15, 16). After stimulation of G protein-coupled receptor (GPCR), RKIP dissociates from Raf-1 and associates with and inhibits GRK-2, a major feedback inhibitor of GPCR (17). The signaling from Ras to Raf-1 is also negatively regulated by Spred and its homologue Sprouty4 (18, 19), but such regulation is not associated with changes in the spatial distribution of Raf-1.

We demonstrate here that a previously uncharacterized Golgi-anchored membrane protein, which we named RKTG (Raf kinase trapping to Golgi), binds Raf-1, translocates Raf-1 into the Golgi apparatus, inhibits Raf-1 activation, reduces association of Raf-1 with Ras and MEK, and blocks the ERK pathway. Our results from both *in vitro* and *in vivo* studies indicate that RKTG is a spatial regulator of Raf kinase and plays a critical role in the regulation of the Ras/Raf/MEK/ERK signaling cascade.

Results and Discussion

RKTG Is a Seven-Transmembrane Protein That Inhibits ERK Signaling. We cloned human RKTG as a close homologue to the adiponectin receptors AdipoR1 and AdipoR2 (20), which are membrane receptors for adiponectin. Adiponectin plays an important role in the regulation of energy and glucose metabolism (21). RKTG was originally named PAQR3 (progestin and adipoQ receptor 3) with uncharacterized function (22). The human RKTG protein contains 311 amino acid residues (Fig. 1*A*). Hydrophobicity analysis indicated that RKTG contained seven transmembrane domains (Fig. 1*A*). Using the structure of AdipoR1 and AdipoR2 as a prototype (20), we hypothesize that RKTG is topologically different from classical GPCRs in that the N-terminal region is localized at the side of cytoplasm. We analyzed the tissue-expression profile of RKTG by RT-PCR in mouse tissues and found that RKTG has higher expression levels in kidney, brain, testis, and liver than in other tissues (Fig. 1*B*).

To find the potential function of RKTG, we analyzed its regulation on a few well characterized signaling pathways. As a result, we found that RKTG was able to negatively regulate ERK signaling. In HEK293T cells, overexpression of RKTG was able to markedly reduce the phosphorylation level of ERK induced by EGF (Fig. 1*C*). Consistently, phosphorylation of the 90-kDa ribosomal S6 kinase (p90RSK), a ERK substrate in the cytoplasm (23), was also inhibited by RKTG. However, overexpression of adiponectin receptor 1 (AdipoR1), a close homologue of RKTG, could not affect EGF-mediated activation of ERK and p90RSK. To further analyze the cellular effect of RKTG, we used PC12 pheochromocytoma cell as a model to investigate the inhibitory effect of RKTG on ERK activation (24). Nerve growth factor (NGF) is able to induce extended activation of ERK in PC12 cells and leads to cell differentiation manifested as neurite outgrowth (25). We found that expression of RKTG strongly inhibited NGF-induced differentiation of PC12 cells [Fig. 1*D* and the supporting information (SI)],

Author contributions: L.F. and Y.C. designed research; L.F., X.X., Q.D., X.L., J.H., F.F., and W.L. performed research; L.F., Z.W., and Y.C. analyzed data; and L.F. and Y.C. wrote the paper.

The authors declare no conflict of interest.

This article is a PNAS Direct Submission.

Abbreviations: RKTG, Raf kinase trapping to Golgi; NGF, nerve growth factor; MEF, mouse embryonic fibroblast.

*To whom correspondence should be addressed at: Institute for Nutritional Sciences, Shanghai Institutes for Biological Sciences, Chinese Academy of Sciences, 294 Taiyuan Road, Shanghai 200031, China. E-mail: ychen3@sibs.ac.cn.

This article contains supporting information online at www.pnas.org/cgi/content/full/0701298104/DC1.

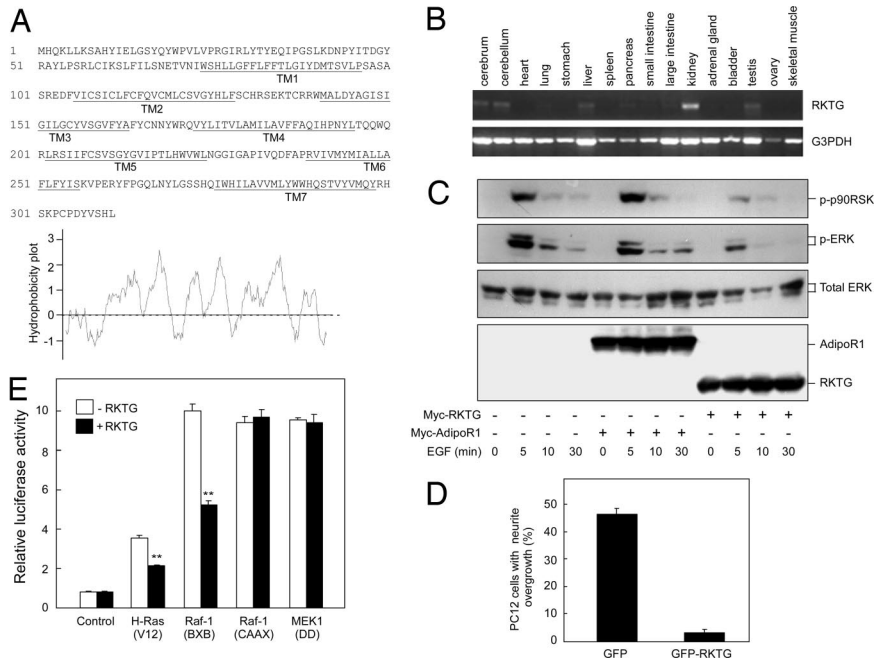

Fig. 1. Structure, tissue expression, and effect on ERK signaling of RKTG. (*A*) Amino acid sequence of human RKTG and hydrophobicity analysis. The locations of predicted seven-transmembrane (TM) domains are underlined. (*B*) Tissue-expression pattern of RKTG. Total RNA was isolated from different mouse tissues as indicated and used in RT-PCR with primers specific for RKTG and G3PDH. (*C*) Inhibition of EGF-induced ERK and p90RSK phosphorylation by RKTG. HEK293T cells were transiently transfected with Myc-tagged AdipoR1 or RKTG as indicated and then treated with EGF (100 ng/ml) for various amounts of time. Total cell lysate was used in the detection of phosphorylated ERK, phosphorylated p90RSK, total ERK, and Myc-tagged proteins by Western blotting. (*D*) RKTG inhibits NGF-induced neuritogenesis in PC12 cells. PC12 cells were transfected with GFP control or GFP-RKTG fusion plasmid. The cells were cultured in the presence of NGF (50 ng/ml) for 48 h and then examined by fluorescence microscopy. Cells with processes longer than twice the diameter of the cell body were considered to be positive for neurite outgrowth. The graph data are shown as the mean ± SD from three independent experiments. (*E*) Regulation of Elk-1-mediated transcriptional response by RKTG. HEK293T cells were transiently transfected with the constitutively active constructs H-Ras(V12), Raf-1(BXB), Raf-1(CAAX), and MEK1(DD) as indicated. The Elk-1-mediated transcriptional response was analyzed as described (39). A renilla luciferase vector was used to monitor the transfection efficiency. The whole-cell lysate was used in a dual luciferase assay, and the fold change of luciferase activity is shown as the mean ± SD. **, $P < 0.01$ (by Student's *t* test).

providing further evidence that RKTG is able to antagonize ERK activation.

To explore how RKTG inhibits ERK activation, we performed a reporter assay that measures the transcriptional activity of Elk-1, a nuclear target of ERK. Various constitutively active components of the Ras/Raf/MEK pathway were used to activate Elk-1 transactivation. They included H-Ras-V12, Raf-1(BXB), which only contains the Raf-1 kinase domain (26), Raf-1(CAAX), which is constitutively targeted to plasma membrane by fusing Raf-1 with the C terminus of H-Ras (27), and MEK1(DD) (28). As shown in Fig. 1*E*, all of these proteins stimulated a Elk-1-mediated transcriptional response. Interestingly, RKTG inhibited Elk-1 transactivation by H-Ras-V12 and Raf-1(BXB) but not by Raf-1(CAAX) and MEK1(DD) (Fig. 1*E*). This observation indicates that RKTG inhibits ERK signaling downstream or at the level of Raf-1 but upstream of MEK.

RKTG Changes the Subcellular Localization of Raf-1 to the Golgi Apparatus. We next investigated the subcellular distribution of RKTG. We first analyzed the localization of endogenous RKTG with a specific RKTG antibody (see the SI). Interestingly, immunofluorescent analysis of endogenous RKTG in HEK293T cells revealed a staining pattern that overlapped with two Golgi markers, Golgin-97 and GM130 (Fig. 2*A*). Meanwhile, a control experiment with preimmune rabbit serum resulted in no specific staining (data not shown). The Golgi localization of RKTG was confirmed by exogenously expressed RKTG that was fused to GFP in HeLa cells (Fig. 2*B*). The subcellular distribution pattern of RKTG was the same when using GFP, HA, or Myc tags at the N terminus in several cell lines (data not shown). Collectively, these results suggest that RKTG is a Golgi protein.

Based on our observation in Fig. 1*E*, we hypothesized that RKTG may affect the Ras/Raf/MEK/ERK pathway at the level of Raf. Under unstimulated condition, Raf-1 was diffusely distributed in the cytoplasm. EGF treatment was able to translocate a portion of Raf-1 to the plasma membrane (Fig. 2*C*, first row) as a result of recruitment by GTP-bound Ras (29, 30). Consistently, the membrane-localized Raf-1 was colocalized with H-Ras (Fig. 2*C*, second row), similar to previous reports (31). Intriguingly, when cotransfected with RKTG, the majority of Raf-1 was translocated to the Golgi apparatus shown as almost complete colocalization with RKTG (Fig. 2*C*, third row). The colocalization of Raf-1 with RKTG was maintained after 30 min of EGF stimulation (Fig. 2*C*, fourth row). On the other hand, RKTG could not change the localization of membrane-bound Raf-1(CAAX) (data not shown), consistent with our observation that RKTG inhibited Raf-1(BXB)-induced but not Raf-1(CAAX)-induced Elk-1 activation (Fig. 1*E*). Furthermore, we investigated the colocalization of Raf-1 with RKTG by three-color confocal analysis. HeLa cells were cotransfected with Raf-1 and RKTG, and different colors were used to label Raf-1, RKTG, and the Golgi. As shown in Fig. 2*D*, the majorities of Raf-1 and RKTG were colocalized at the Golgi apparatus. In addition, the spatial regulation of RKTG on the Ras/Raf/MEK pathway appeared to be specific for Raf, because RKTG had no impact on H-Ras translocation to the membrane ruffles when treated with EGF (see the SI). RKTG was not colocalized with MEK1 either (see the SI). Taken together, these observations suggest that RKTG is exclusively localized at the Golgi apparatus and may inhibit ERK activation by specifically sequestering cytoplasmic Raf-1 at the Golgi apparatus and thereby attenuate ERK signaling.

Interaction of RKTG with Raf-1. Taking into consideration that RKTG is able to trap Raf-1 to the Golgi apparatus, we analyzed whether Raf-1 interacts with RKTG. When Raf-1 and RKTG were coexpressed, RKTG could interact with Raf-1, and such interaction was slightly increased upon EGF treatment (Fig. 3*A*). We next investigated the interaction of endogenous Raf-1 with endogenous RKTG. As shown in Fig. 3*B*, the anti-Raf-1 antibody but not mouse IgG was able to coprecipitate endogenous RKTG. These data, therefore, indicate that RKTG could physically associate with Raf-1. On the other hand, we could not detect RKTG interaction with Ras or MEK by coimmunoprecipitation assay (data not shown), consistent with our results from colocalization studies.

We also examined whether RKTG would interfere with Raf-1 activation. Ser-338 is a key phosphorylation site in Raf-1, and this phosphorylation regulates both autoinhibition of Raf-1 and the

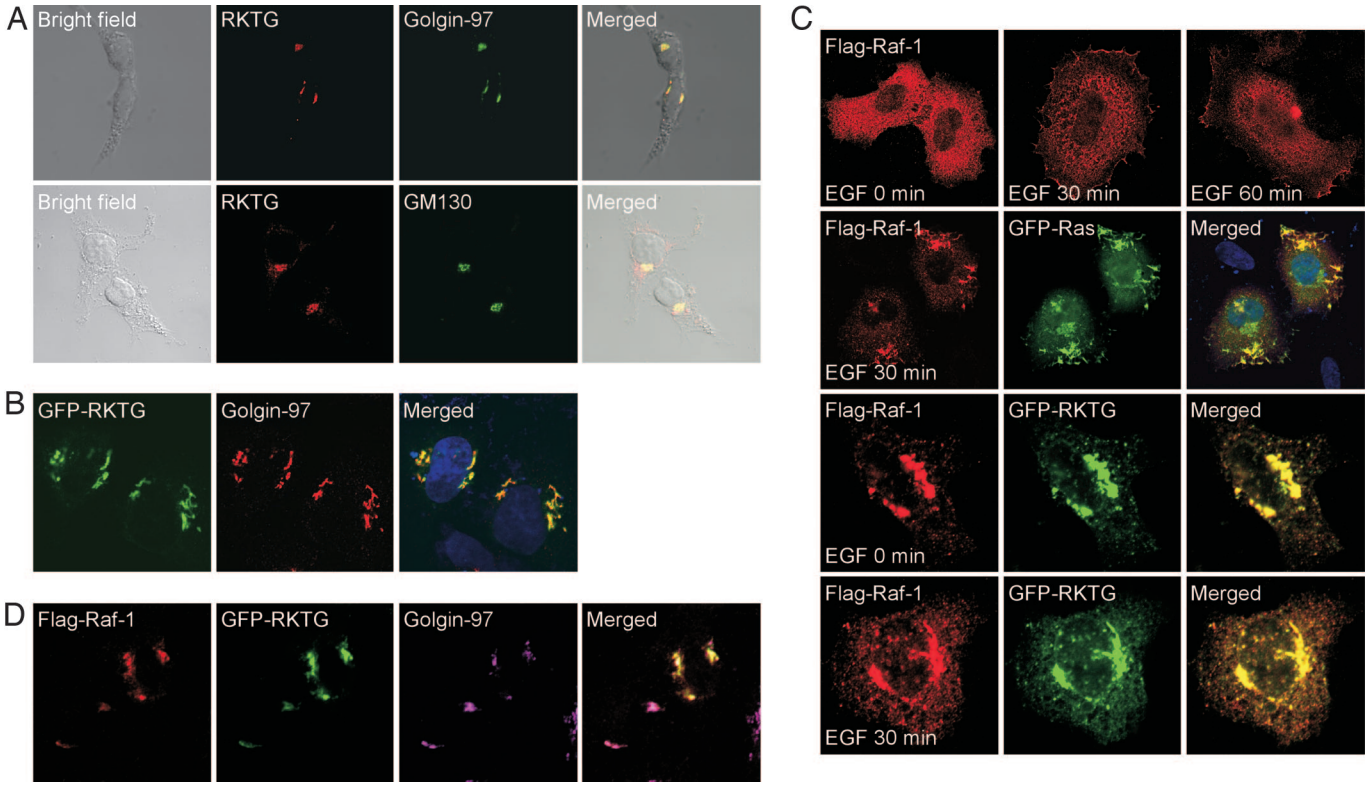

Fig. 2. Raf-1 colocalizes with RKTG at the Golgi apparatus. (*A*) Endogenous RKTG is localized at the Golgi. HEK293T cells were stained with affinity-purified anti-RKTG antibody (red) and the Golgi markers Golgin-97 (green) or GM130 (green) as indicated. The cells were fixed and used in confocal analysis. The bright fields are also shown to reveal the overall structure of the cells. (*B*) Ectopically expressed RKTG is localized at the Golgi. HeLa cells were transfected with GFP-RKTG fusion plasmid. The Golgi was labeled by Golgin-97 (red), and the cell nuclei were stained with Hoechest 33342 (blue). (*C*) Colocalization of RKTG with Raf-1. HeLa cells were transfected with the plasmid as indicated and followed by serum starvation. EGF treatment induced membrane localization of Raf-1 (first row), as well as formation of membrane ruffles that contained Ras and Raf-1 (second row). RKTG coexpression changed the localization of Raf-1 from cytosol to the Golgi in the absence (third row) or presence (fourth row) of EGF. The change of the subcellular localization of Raf-1 by RKTG blocked membrane translocation of Raf-1 upon EGF treatment (bottommost row). (*D*) Confocal immunofluorescence microscopy of HeLa cells with triple colors. The cells were transfected with Flag-tagged Raf-1 and GFP-RKTG fusion construct and then labeled with a polyclonal antibody against Flag-tagged Raf-1 (red) and a monoclonal antibody against Golgin-97 (purple). Note that the merged image shows a significant overlapping of the three signals.

interaction of Raf-1 with MEK (32, 33). We found that RKTG overexpression inhibited Raf-1 Ser-338 phosphorylation in response to EGF (Fig. 3*C*). Because growth-factor-stimulated Ser-338 phosphorylation occurs at the plasma membrane (34), this result is consistent with our observation that RKTG blocks membrane translocation of Raf-1 upon EGF stimulation (Fig. 2*C*).

Because RKTG could interact with Raf-1 and trap Raf-1 to the Golgi, we hypothesized that the RKTG/Raf-1 interaction might compete for the interaction of Raf-1 with Ras and MEK. We addressed this issue by coimmunoprecipitation assay with various expression levels of RKTG. The interaction of Raf-1 with RKTG was increased upon increasing expression of RKTG (Fig. 3*D*, third row). Intriguingly, increasing expression of RKTG led to decreasing interaction of Raf-1 with endogenous Ras and endogenous MEK1 simultaneously (Fig. 3*D*, first and second rows). The RKTG family protein AdipoR1, however, could not affect the interaction of Raf-1 with Ras and MEK1 (Fig. 3*D*). These data suggest that RKTG, through sequestering Raf-1 at the Golgi, reduces the accessibility of Raf-1 to Ras and MEK and consequently blocks the signaling from Ras to ERK.

The N Terminus of RKTG Is Required for Golgi Localization and Raf-1 Interaction. To define the region of RKTG that is necessary for Raf-1 interaction, we constructed both N- and C-terminal truncation mutants of RKTG. Deletion of the N-terminal 71 hydrophilic amino acid residues (ΔN71) located upstream of the first transmembrane domain led to complete loss of Golgi localization (Fig. 4*A Top*). Such deletion appeared to change the localization of RKTG to endothelium reticulum as the deleted protein was colocalized with endothelium reticulum marker GFP-IRE1-α (35) (Fig. 4*A Middle*). These findings indicate that the N terminus may contain Golgi targeting signal for RKTG. Consistently, the N-terminal truncated RKTG was no longer colocalized with Raf-1 (Fig. 4*A Bottom*). In addition, deletion of the N-terminal 71 amino acids caused a loss of Raf-1 binding ability, whereas interaction with Raf-1 was retained after the deletion of the C-terminal 20 amino acids of RKTG (RKTGΔC20) (Fig. 4*B*). Furthermore, the full-length RKTG and RKTGΔC20, but not RKTGΔN71, could inhibit Raf-1(BXB)-induced Elk-1 transactivation (Fig. 4*C*). Taken together, these observations indicate that the N-terminal region of RKTG is necessary for Golgi localization, Raf-1 association, and ERK inhibition.

***In Vivo* Deletion of RGTG Enhances ERK Signaling.** Our studies so far have demonstrated that RKTG could inhibit ERK signaling by sequestering Raf-1 to the Golgi apparatus via interaction with Raf-1 and alleviating the interaction of Raf-1 with Ras and MEK. We next analyzed the *in vivo* function of RKTG by generation of RKTG knockout mice. Mouse and human RKTG share 97% identity at the amino acid level. The mouse RKTG gene contains seven exons, and the second exon was targeted for deletion (Fig. 5*A*). We successfully deleted exon 2 in the mouse (see the SI), and such deletion would only leave the first 62 aa intact because the deletion (163 bp in

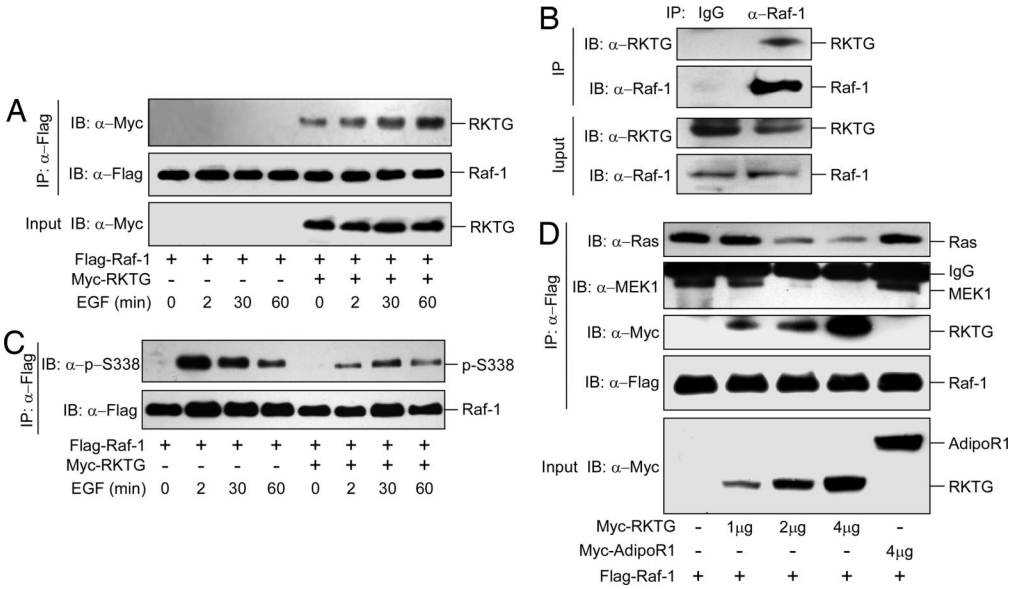

Fig. 3. Interaction of RKTG with Raf-1. (*A*) Interaction of overexpressed RKTG with Raf-1. HEK293T cells were transiently transfected with Flag-tagged Raf-1 and Myc-tagged RKTG as indicated. After transfection, the cells were serum-starved for 16 h and then treated with EGF (100 ng/ml) for the indicated times. The cell lysate was used in immunoprecipitation (IP) and immunoblotting (IB) with the antibodies as indicated. (*B*) Interaction of endogenous RKTG with endogenous Raf-1. Total cell lysates of HEK293T cells were subjected to immunoprecipitation with an anti-Raf-1 antibody followed by immunoblotting with an antibody against human RKTG. Mouse IgG was used as a negative control. (*C*) RKTG inhibits Raf-1 activation. HEK293T cells were transiently transfected with Flag-tagged Raf-1 and Myc-tagged RKTG. The Flag-tagged Raf-1 was immunoprecipitated after EGF stimulation for indicated times. Immunoblotting was performed by using the antibodies as indicated. (*D*) RKTG interferes with the interaction of Raf-1 with Ras and MEK1. HEK293T cells were transiently transfected with the plasmid as indicated. The Flag-tagged Raf-1 was immunoprecipitated, and the Raf-1-associated RKTG, Ras, and MEK1 were analyzed by immunoblotting.

length) causes frameshift of downstream sequences and results in loss of all of the transmembrane domains of RKTG. The RKTG-deleted mice were born alive and had no apparent phenotype up to 6 months of age on the current mixed genetic background. We first analyzed the basal activity of the ERK pathway in different tissues. In both brain and liver, the basal ERK phosphorylation level was profoundly increased in female RKTG$^{-/-}$ mice (Fig. 5*B Left*). Interestingly, the ERK phosphorylation level was also elevated in male RKTG$^{+/-}$ mice (Fig. 5*B Right*), indicative of a sex difference in the regulation of ERK signaling by RKTG. Furthermore, we investigated EGF-induced ERK phosphorylation in mouse embryonic fibroblast (MEF). EGF treatment induced a rapid ERK phosphorylation in MEF$^{+/+}$ with a maximal level at 5 min, and the signal was almost completely attenuated to the basal level at 30 min (Fig. 5*C*). In MEF$^{-/-}$, however, the maximal stimulation of ERK phosphorylation upon EGF treatment was extended to 30 min and remained active at 100 min (Fig. 5*C*). These data, therefore, reveal that the EGF-induced ERK phosphorylation was both enhanced and prolonged in RKTG-deficient MEFs, indicating that RKTG regulates both the intensity and duration of ERK activation upon EGF treatment *in vivo*. Moreover, because EGF mediates activation of both AKT and ERK pathways (36), we also examined AKT activation in MEFs. Unlike the observation with ERK phosphorylation, the EGF-induced phosphorylation of AKT was not enhanced in RKTG-null cells (SI), indicating that RKTG mainly affects the Ras–Raf–ERK pathway but not the Ras–PI3K–AKT pathway.

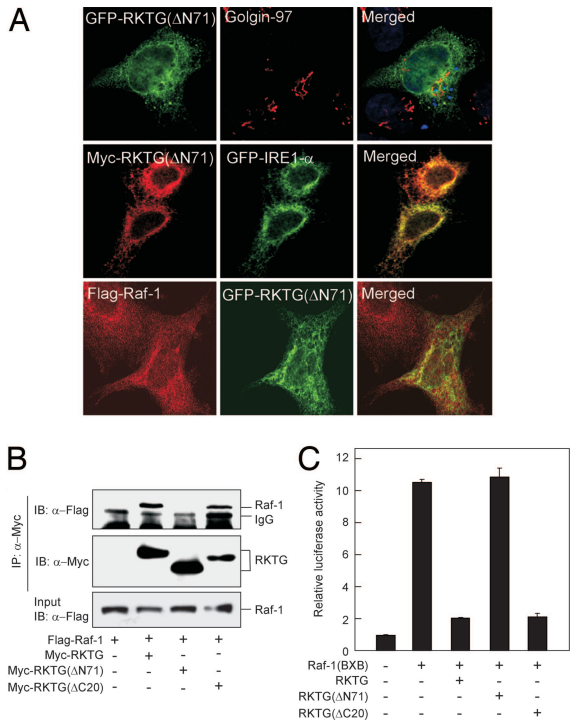

Fig. 4. RKTG N terminus is needed for interaction with Raf-1. (*A*) Colocalization studies of RKTGΔN71 in HeLa cells. (*Top*) GFP-RKTGΔN71 fusion protein with the Golgi marker Golgin-97. (*Middle*) Myc-tagged RKTGΔN71 with an ER marker, GFP-IRE1-α. (*Bottom*) GFP-RKTGΔN71 with Flag-tagged Raf-1. (*B*) Interaction of RKTG truncation mutants with Raf-1. HEK293 cells were transfected with the plasmids as indicated, and the cell lysate was used in immunoprecipitation (IP) and immunoblotting (IB) with the indicated antibodies. (*C*) Effects of the N- and C-terminal RKTG deletions on Raf-1(BXB)-induced Elk-1 transactivation. The luciferase assay was performed as described in Fig. 1*E*.

RKTG Is a Spatial Regulator of Raf Kinase. The pathway from Ras through Raf and MEK to ERK regulates many fundamental cellular processes. How this pathway integrates complicated extracellular signals and determines distinct biological outcomes has recently drawn much attention. The strength and duration of ERK signaling, especially the latter, has been proved to be very important in the regulation of cell fate determination (37). In PC12 cells, only sustained activation of ERK signaling stimulated by NGF precedes the differentiation of these cells, and transient activation caused by EGF or insulin only results in a weak proliferative response (38). The Raf/MEK/ERK kinase module is able to act as a molecular switch *in vivo*, but the input sensitivity of the module is determined by subcellular localization of the MAPK components (5). In T lymphocyte, Ras/MAPK signaling in different subcellular compartments leads to distinct output that controls the threshold of thymic selection (12).

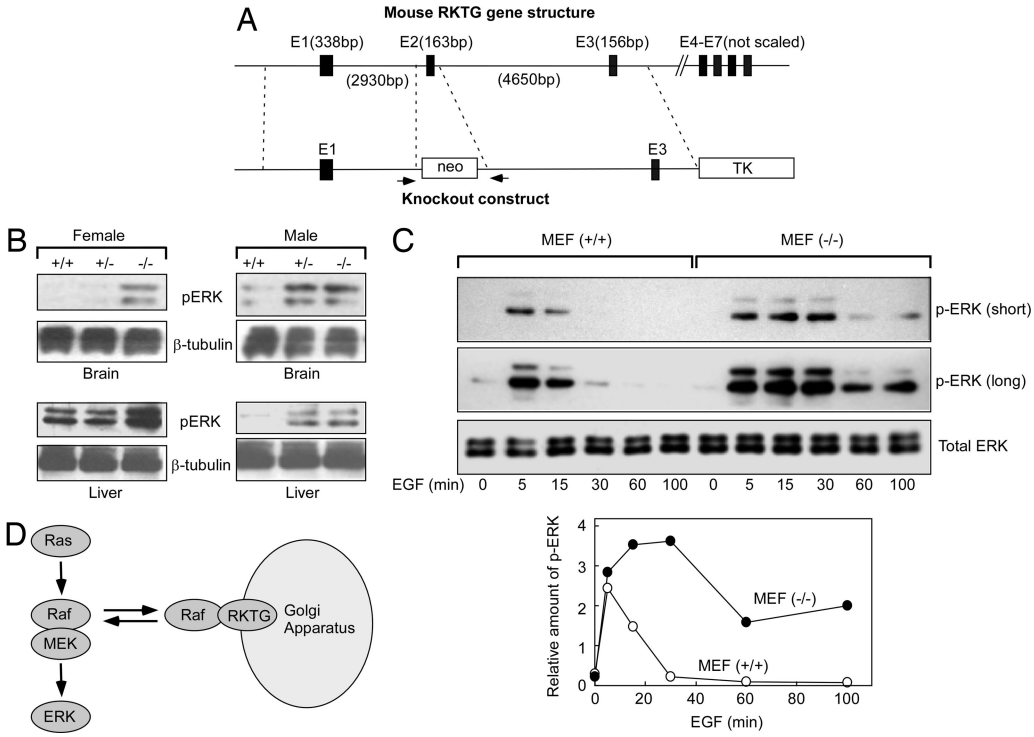

Fig. 5. Studies with RKTG knockout mouse. (*A*) Schematic illustration of the mouse RKTG gene structure and the RKTG knockout construct. The seven exons (E1–E7) are marked, and the nucleotide lengths for some of the exons and introns are also shown. Homologous recombination (in the regions marked by dotted lines) would cause deletion of exon 2. The arrows indicate the position of PCR primers used for genotyping the mouse. (*B*) The basal ERK phosphorylation level is increased in tissues from RKTG-deleted mouse. Brain and liver were isolated from both male and female mice. The basal phosphorylation level of ERK and the loaded protein levels were determined by Western blotting as indicated. (*C*) EGF-induced ERK phosphorylation is enhanced and prolonged in RKTG-deleted MEF. MEFs isolated from the mouse embryos were cultured in serum-starved medium for 6 h and then treated with EGF treatment (100 ng/ml). The total cell lysate was used in immunoblotting. Both short and long exposures for ERK phosphorylation are shown. The relative amount of ERK phosphorylation as compared with total ERK level is shown in the graph. (*D*) A model for the function of RKTG. RKTG interacts with cytoplasmic Raf-1 and sequesters Raf-1 in the Golgi apparatus, thereby attenuating the signaling from Ras to MEK and ERK.

Our results reveal a previously uncharacterized type of spatial regulator of Raf kinase (Fig. 5*D*). RKTG is a seven-transmembrane protein exclusively localized at the Golgi apparatus. Through interaction with Raf-1, RKTG sequesters Raf-1 to the Golgi apparatus and blocks the interaction of Raf-1 with Ras and MEK, thus insulating the signaling from Ras to MEK/ERK. As a spatial regulator, RKTG acts as a Golgi-anchoring protein of Raf-1 rather than a scaffold, because RKTG does not bind other members of the MAPK module. The function of RKTG as a negative regulator in the MAPK pathway appears to be both sufficient and necessary. Overexpression of RKTG significantly inhibits EGF-induced ERK and p90RSK activation, antagonizes NGF-mediated differentiation of PC12 cells, and blocks Ras- and Raf-1-stimulated transactivation of Elk-1. On the other hand, deletion of RKTG results in up-regulation of ERK activation in both mouse tissues and MEFs. Importantly, upon EGF stimulation, the RKTG-deleted MEFs have a sustained ERK signaling (Fig. 5*C*). Such prolonged ERK activation can be considered as a distinct signal output. In other words, the same input in ERK signaling could lead to different output signals that depend on the cellular amount of RKTG. In this regard, the duration and intensity of intracellular ERK signaling could be fine-tuned by the relative expression level of RKTG in a cell. Considering the importance of RKTG in ERK signaling, the next challenge would be to elucidate the physiological outcomes and molecular mechanisms underlying the regulation of RKTG.

Materials and Methods

Plasmid Construction. The full-length human RKTG cDNA (GenBank entry AY424281) and the human AdipoR1 cDNA were isolated from HEK293T cells by RT-PCR and confirmed by DNA sequencing. RKTG and its deletion mutants as well as AdipoR1 were subcloned into the mammalian expression vector pCS2+MT with six Myc tags at the N terminus. RKTG and H-Ras were cloned into pEGFP-C1 (Clontech, Mountain View, CA) to fuse with an enhanced green fluorescence protein at the N terminus. The Elk-reporter system contains pSG-Gal4-Elk1 and pG5.EfΔlux3 (39). The constitutively active H-Ras-V12, Raf-1(BxB) and MEK1(DD) were kindly provided by Susanne Weg-Remers (Institut für Toxikologie und Genetik, Karlsruhe, Germany) (39); Flag-tagged Raf-1 was kindly provided by Dong Xie (Chinese Academy of Sciences); GFP-IRE1-α was from Yong Liu (Chinese Academy of Sciences); HA-tagged MEK1 was from Natalie G. Ahn (University of Colorado, Boulder); and Raf-1(CAAX) was from Philip J. S. Stork (Oregon Health and Science University, Portland).

Cell Culture and Transfection. HEK293T, HeLa, and MEF cells were cultured in DMEM containing 10% FBS. Rat pheochromocytoma-derived PC12 cells were cultured in DMEM/F-12 medium containing 10% horse serum and 5% FBS. For PC12 differentiation, the culture medium was changed to DMEM/F-12 medium containing 1% horse serum and 50 ng/ml NGF. Transient transfection was performed with the polyethylenimine (PEI) method for HEK293T and HeLa cells and Lipofectamine 2000 (Invitrogen, Carlsbad, CA) for PC12 cells according to the manufacturer's instructions.

Luciferase Assay. The luciferase assay to analyze Elk-1-mediatd transcriptional response was performed as previously described (39). Twelve hours after transfection, the cells were serum-

starved for 16 h before harvesting. The luciferase activity was measured by a luciferase assay kit (KenReal, Shanghai, China) with a luminometer (Berthold Technologies, Bad Wildbad, Germany).

Antibodies, Immunoprecipitation, and Immunoblotting. The antibodies were purchased as follows: phospho-ERK1/2, phospho-p90RSK(Ser-380), phospho-AKT(Ser-473), and phospho-c-Raf(Ser-338) were from Cell Signaling Technology (Danvers, MA); monoclonal and polyclonal anti-FLAG antibody were from Sigma–Aldrich (St. Louis, MO); antibodies against Myc, HA, tubulin, Raf-1, and total ERK1/2 were from Santa Cruz Biotechnology (Santa Cruz, CA); pan-Ras and MEK1 antibody were from BD Biosciences Transduction Laboratories (Lexington, KY); Golgin-97 monoclonal antibody, Alexa Fluor 488 donkey anti-mouse IgG, Alexa Fluor 546 goat anti-mouse, rabbit IgG, and Hoechst 33342 were from Molecular Probes (Eugene, OR); and Cy5-labeled goat anti-mouse IgG was from GE Healthcare (Chalfont St. Giles, U.K.). The polyclonal RKTG antibodies was generated by rabbit immunization with a His-tagged fusion protein that contains three hydrophilic regions of human RKTG (amino acid residues 2–76, 254–278, and 296–310). The antibodies were affinity-purified against recombinant GST-RKTG fusion protein coupled to Glutathione Sepharose 4B according to the manufacturer's instructions (GE Healthcare). The cells were lysed in a buffer containing 20 mM Tris·HCl (pH 7.5), 150 mM NaCl, 5 mM EGTA, and 1% Nonidet P-40 with a mixture of protease inhibitors and phosphotase inhibitor (Sigma–Aldrich) before immunoprecipitation and immunoblotting assays.

Confocal Microscopy. Cells were grown on glass coverslips. Forty-eight hours after transfection, the cells were fixed with 4% paraformaldehyde in PBS, permeabilized with 0.1% Triton X-100 in PBS for 10 min, and incubated with primary and secondary antibodies, sequentially. Confocal images were captured with an LSM 510 confocal microscope with a 64 × 1.4 N.A. apochromat objective (Zeiss, Jena, Germany). The 488 line of an argon laser was used for fluorescence excitation of EGFP and Alexa 488-conjugated antibodies. A helium/neon laser (543 nm) was used for excitation of Alexa 546-conjugated antibodies, and 633 nm was used for excitation of Cy5-conjugated antibody. After data acquisition, red/green/blue (RGB) images were processed by using LSM 510 software.

Generation of RKTG Knockout Mouse and Preparation of MEF. The RKTG knockout construct was made with a bacteria-based homologous recombination method (40) in which the second exon of the mouse RKTG gene was replaced by a neomycin-selectable cassette. After electroporation of the knockout construct into ES cells and screening with Southern blotting, three independent ES cell clones that carried the targeting construct were injected into C57BL/6J blastocysts. Male chimeric founders were crossed to C57BL/6J females to generate $RKTG^{+/-}$ mice that were used to produce homozygous $RKTG^{-/-}$ mice. For genotyping, mouse-tail DNA was amplified with primers 5′-GCTGTCACTCCCAGGATTATTG-3′ and 5′-CCTGTGCAAGCATTCCTGAC-3′ as illustrated in the SI. Total RNA isolated from the liver was used to analyze the expression status of RKTG for each genotype by RT-PCR with primers that specifically amplify individual regions. MEFs were prepared from day-13.5 embryos derived from a cross between $RKTG^{+/-}$ mice. The head and internal organs were removed, and the torso was minced and dispersed in 0.1% trypsin. The cells were grown for two population doublings before freezing. The genotype of MEF was identified by genomic PCR, and the expression status of RKTG was confirmed by RT-PCR.

We thank Drs. Susanne Weg-Remers, Natalie G. Ahn, Philip J. S. Stork, Dong Xie, and Yong Liu for providing the plasmids. This work was supported by Chinese Academy of Sciences (One Hundred Talents program and the Knowledge Innovation Program) Grant KSCX1-YW-02 (to Y.C.), National Natural Science Foundation of China Grants 30588002 and 30470870 (to Y.C.), Science and Technology Commission of Shanghai Municipality Grants 04DZ14007 and 05DJ14009 (to Y.C.), and Ministry of Science and Technology of China Grants 2006CB943902 and 2007CB947100 (to Y.C.).

1. Wellbrock C, Karasarides M, Marais R (2004) *Nat Rev Mol Cell Biol* 5:875–885.
2. Kolch W (2005) *Nat Rev Mol Cell Biol* 6:827–837.
3. Rapp UR, Gotz R, Albert S (2006) *Cancer Cell* 9:9–12.
4. Mor A, Philips MR (2006) *Annu Rev Immunol* 24:771–800.
5. Harding A, Tian T, Westbury E, Frische E, Hancock JF (2005) *Curr Biol* 15:869–873.
6. Morrison DK (2001) *J Cell Sci* 114:1609–1612.
7. Luttrell LM, Roudabush FL, Choy EW, Miller WE, Field ME, Pierce KL, Lefkowitz RJ (2001) *Proc Natl Acad Sci USA* 98:2449–2454.
8. Choy E, Chiu VK, Silletti J, Feoktistov M, Morimoto T, Michaelson D, Ivanov IE, Philips MR (1999) *Cell* 98:69–80.
9. Chiu VK, Bivona T, Hach A, Sajous JB, Silletti J, Wiener H, Johnson RL, II, Cox AD, Philips MR (2002) *Nat Cell Biol* 4:343–350.
10. Rocks O, Peyker A, Bastiaens PI (2006) *Curr Opin Cell Biol* 18:351–357.
11. Bivona TG, Perez De Castro I, Ahearn IM, Grana TM, Chiu VK, Lockyer PJ, Cullen PJ, Pellicer A, Cox AD, Philips MR (2003) *Nature* 424:694–698.
12. Daniels MA, Teixeiro E, Gill J, Hausmann B, Roubaty D, Holmberg K, Werlen G, Hollander GA, Gascoigne NR, Palmer E (2006) *Nature* 444:724–729.
13. Teis D, Wunderlich W, Huber LA (2002) *Dev Cell* 3:803–814.
14. Torii S, Kusakabe M, Yamamoto T, Maekawa M, Nishida E (2004) *Dev Cell* 7:33–44.
15. Yeung K, Seitz T, Li S, Janosch P, McFerran B, Kaiser C, Fee F, Katsanakis KD, Rose DW, Mischak H, *et al.* (1999) *Nature* 401:173–177.
16. Yeung K, Janosch P, McFerran B, Rose DW, Mischak H, Sedivy JM, Kolch W (2000) *Mol Cell Biol* 20:3079–3085.
17. Lorenz K, Lohse MJ, Quitterer U (2003) *Nature* 426:574–579.
18. Wakioka T, Sasaki A, Kato R, Shouda T, Matsumoto A, Miyoshi K, Tsuneoka M, Komiya S, Baron R, Yoshimura A (2001) *Nature* 412:647–651.
19. Sasaki A, Taketomi T, Kato R, Saeki K, Nonami A, Sasaki M, Kuriyama M, Saito N, Shibuya M, Yoshimura A (2003) *Nat Cell Biol* 5:427–432.
20. Yamauchi T, Kamon J, Ito Y, Tsuchida A, Yokomizo T, Kita S, Sugiyama T, Miyagishi M, Hara K, Tsunoda M, *et al.* (2003) *Nature* 423:762–769.
21. Kadowaki T, Yamauchi T, Kubota N, Hara K, Ueki K, Tobe K (2006) *J Clin Invest* 116:1784–1792.
22. Tang YT, Hu T, Arterburn M, Boyle B, Bright JM, Emtage PC, Funk WD (2005) *J Mol Evol* 61:372–380.
23. Sturgill TW, Ray LB, Erikson E, Maller JL (1988) *Nature* 334:715–718.
24. Greene LA, Tischler AS (1976) *Proc Natl Acad Sci USA* 73:2424–2428.
25. Marshall CJ (1995) *Cell* 80:179–185.
26. Frost JA, Alberts AS, Sontag E, Guan K, Mumby MC, Feramisco JR (1994) *Mol Cell Biol* 14:6244–6252.
27. Carey KD, Watson RT, Pessin JE, Stork PJ (2003) *J Biol Chem* 278:3185–3196.
28. Franklin CC, Kraft AS (1995) *Oncogene* 11:2365–2374.
29. Stokoe D, Macdonald SG, Cadwallader K, Symons M, Hancock JF (1994) *Science* 264:1463–1467.
30. Mineo C, James GL, Smart EJ, Anderson RG (1996) *J Biol Chem* 271:11930–11935.
31. Bar-Sagi D, Feramisco JR (1986) *Science* 233:1061–1068.
32. Xiang X, Zang M, Waelde CA, Wen R, Luo Z (2002) *J Biol Chem* 277:44996–45003.
33. Tran NH, Frost JA (2003) *J Biol Chem* 278:11221–11226.
34. Diaz B, Barnard D, Filson A, MacDonald S, King A, Marshall M (1997) *Mol Cell Biol* 17:4509–4516.
35. Wang XZ, Harding HP, Zhang Y, Jolicoeur EM, Kuroda M, Ron D (1998) *EMBO J* 17:5708–5717.
36. Wennstrom S, Downward J (1999) *Mol Cell Biol* 19:4279–4288.
37. Murphy LO, Blenis J (2006) *Trends Biochem Sci* 31:268–275.
38. Cowley S, Paterson H, Kemp P, Marshall CJ (1994) *Cell* 77:841–852.
39. Weg-Remers S, Ponta H, Herrlich P, Konig H (2001) *EMBO J* 20:4194–4203.
40. Cotta-de-Almeida V, Schonhoff S, Shibata T, Leiter A, Snapper SB (2003) *Genome Res* 13:2190–2194.